Chemistry & Biology
Article

Self-Acylation Properties of Type II Fatty Acid Biosynthesis Acyl Carrier Protein

Ashish Misra,[1] Shailendra Kumar Sharma,[1] Namita Surolia,[2] and Avadhesha Surolia[1,3,*]
[1] Molecular Biophysics Unit, Indian Institute of Science, Bangalore 560012, India
[2] Molecular Biology and Genetics Unit, Jawaharlal Nehru Centre for Advanced Scientific Research, Bangalore 560064, India
[3] National Institute of Immunology, New Delhi 110067, India
*Correspondence: surolia@nii.res.in
DOI 10.1016/j.chembiol.2007.05.013

SUMMARY

Acyl carrier protein (ACP) plays a central role in many metabolic processes inside the cell, and almost 4% of the total enzymes inside the cell require it as a cofactor. Here, we report self-acylation properties in ACPs from *Plasmodium falciparum* and *Brassica napus* that are essential components of type II fatty acid biosynthesis (FAS II), disproving the existing notion that this phenomenon is restricted only to ACPs involved in polyketide biosynthesis. We also provide strong evidence to suggest that catalytic self-acylation is intrinsic to the individual ACP. Mutational analysis of these ACPs revealed the key residue(s) involved in this phenomenon. We also demonstrate that these FAS II ACPs exhibit a high degree of selectivity for self-acylation employing only dicarboxylic acids as substrates. A plausible mechanism for the self-acylation reaction is also proposed.

INTRODUCTION

Acyl carrier protein (ACP) is one of the most abundant proteins present inside the cell, and plays a central role in metabolic processes involving acyl group transfer viz. fatty acid biosynthesis [1], polyketide biosynthesis [2, 3], and nonribosomal peptide synthesis [4, 5]. It also acts as a cofactor for the transfer of fatty acids to the lipid A portion of lipopolysaccharide of Gram-negative bacterial membranes [6], rhizobial capsular polysaccharide biosynthesis [7], and the production of Nod factors in rhizobia [8]. ACPs are small acidic proteins (80–100 amino acids), and can either exist as an integral component of a large fatty acid synthase (FAS) (type I) [9] complex present in mammals, fungi, and certain mycobacteria, or an independent protein, as in type II or dissociative-type fatty acid biosynthesis [1] found in most bacteria, plants, and some apicomplexans [10].

ACP acts as an indispensable cofactor for de novo fatty acid biosynthesis. It is generally expressed in the apo form and is posttranslationally modified to active holo form by the addition of 4′-phosphopantetheine (4′-PP) moiety to an absolutely conserved serine residue. This reaction is catalyzed by holo-ACP synthase (ACPS) or 4′-PP transferase (P-pant transferase) [11, 12]. Growing acyl intermediates and nascent product molecules are covalently tethered to the terminal thiol group of the 4′-PP arm of ACPs during the elongation and modification steps required for the synthesis of the final product.

Owing to the crucial roles of ACPs in metabolism, the high degree of conservation in its primary sequence across all kingdoms is not surprising. The three-dimensional structure of *Escherichia coli* ACP is a prototype of bacterial and plant ACP structures, which is an asymmetric monomer consisting of a three helix bundle and a short fourth helix, all connected by loops along with a structured turn between helices I and II. Helix II is widely believed to be the major recognition helix, and acidic residues present in this helix are involved in protein-protein interactions in both modular polyketide synthase (PKS) [13] and FAS [14]. Although, mutations of these acidic residues in this helix are thought to stabilize the folded conformation, they may alter its interaction with other enzymes [15].

FAS ACPs have an unusual dynamic equilibrium between two conformers [16–18], while only a single conformation is observed in the case of ACP of PKS [19, 20]. Although the significance of these conformations is not clearly understood, it might allow them to interact with enzymes other than those involved in fatty acid synthesis to reversibly direct acyl groups to the active site of these enzymes.

The absence of a discrete malonyl CoA:ACP transacylase (MCAT) in the type II polyketide biosynthesis gene cluster led many groups to propose the involvement of FAS MCAT in polyketide biosynthesis. Later however, Hitchman et al. [21] demonstrated that a variety of type II polyketide synthesis ACPs were subject to non-MCAT-catalyzed acylation in the presence of malonyl-CoA. They showed that these ACPs could also utilize dicarboxylic acids and β-keto acid thiol esters, which are not natural substrates for these enzymes. They also provided strong evidences demonstrating the absence of such a self-acylation process in type II FAS ACPs.

In contrast, studies reported here demonstrate that self-acylation is not inherent to type II PKS ACPs only, but is also shown by certain ACPs involved in type II fatty acid biosynthesis *viz*. *Plasmodium falciparum* ACP and *Brassica napus* chloroplast targeted ACP. However, unlike

the PKS ACPs, the FAS ACPs employ only dicarboxylic acids, such as malonyl-, succinyl-, and glutaryl-CoAs, as substrates, and self-acylation with β-keto acid thioesters for the latter is not observed. Insights into the kinetics of the reactions for both *P. falciparum* ACPs (PfACPs) and *B. napus* ACPs (BnACPs) are reported in these studies. We also demonstrate that mutation of a conserved residue in both PfACP and BnACP compromises the self-acylation property of these ACPs and propose a likely mechanism for the reaction.

RESULTS

Cloning and Expression of BnACP

The BnACP was cloned, overexpressed and purified to homogeneity using nickel-NTA metal affinity chromatography (see Figures S1A–S1C in the Supplemental Data available with this article online). Furthermore, the protein was loaded onto thiopropyl Sepharose 6B column in order to separate apo- and holo-BnACP. The purity of holo-BnACP, as determined by native PAGE at acidic pH, was found to be >95% (Figure S1D). PfACP was purified as described previously [22].

For homology modeling of BnACP, multiple sequence alignment of various ACPs obtained from ClustalW was used as input into MODELER, and *E. coli* butyryl ACP structure was employed as a template. BnACP model exhibited a prototypical ACP structure composed of a four-α-helical bundle, with a central cavity capable of accommodating 4′-PP prosthetic group and the thioester-bound acyl chain (Figures S2A and S2B).

Determination of Self-Acylation Properties of FAS II ACP

Steady-state spectrophotometric kinetics measurements utilizing coupled assays were performed to determine the kinetics as well as specificity of self-acylation behavior for PfACP and BnACP (Figures 1A–1C and Figures S3A–S3C) The experiments demonstrated that, unlike the PKS ACPs, the FAS ACPs utilize only malonyl, succinyl, and glutaryl CoAs, and no activity was observed with acetyl, butyryl, methylmalonyl, and acetoacetyl CoAs (Table 1).

Reduction in the self-malonylation property with increasing concentration of iodoacetamide confirmed that self-malonylation requires a thiol group at the phosphopantetheine arm of ACPs (Figures S4A and S4B).

Mass spectrometry was also employed to confirm the formation of self-acylated products. In the PfACP self-acylation reaction, the mass of the control reaction containing purified holo-PfACP was 9722 ± 1 Da (calculated, 9722 Da), while that of self-malonylated PfACP was 9807 ± 1 Da (calculated, 9807 Da), self-succinylated PfACP was 9823 ± 1 Da (calculated, 9823 Da), and self-glutarylated PfACP was 9837 ± 1 Da (calculated, 9837 Da) (Figures 2A–2D). Similarly, for the BnACP self-acylation reaction, the mass of the control reaction containing purified holo-BnACP was 10,508 ± 1 Da (calculated, 10,508 Da), while that of self-malonylated BnACP was 10,591 ± 2 Da (calculated 10,593 Da), self-succinylated BnACP was 10,607 ± 2 Da (calculated 10,609 Da), and self-glutarylated BnACP was 10,624 ± 1 Da (calculated 10,623 Da) (Figure 2D–2G).

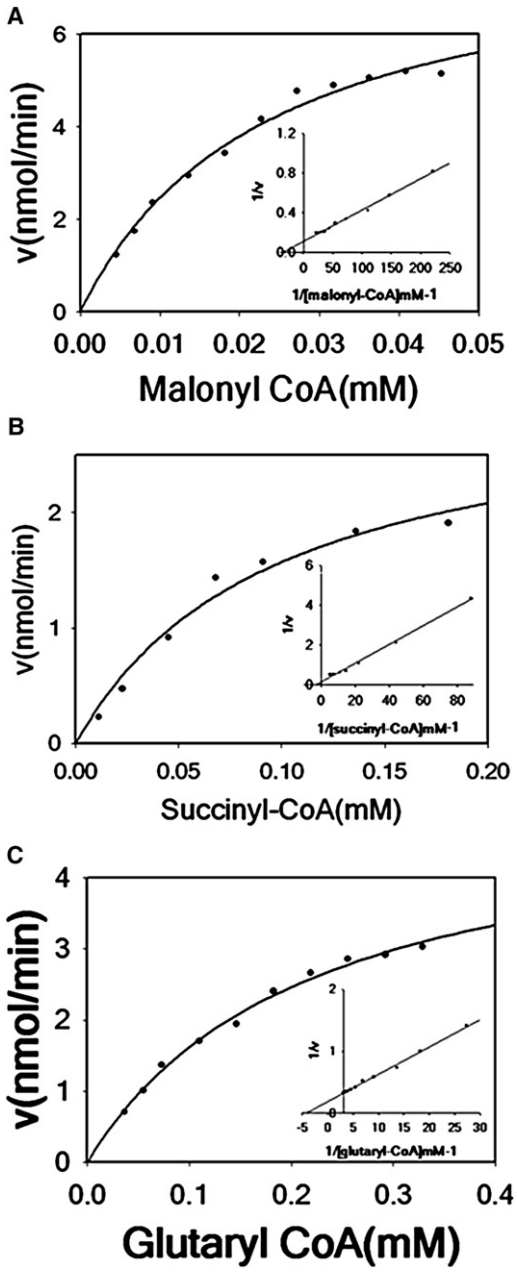

Figure 1. Kinetic Characterization of Self-Malonylation, Self-Succinylation, and Self-Glutarylation of *P. falciparum*

The initial velocities of product formation were determined with increasing concentrations of malonyl-CoA, succinyl-CoA, and glutaryl-CoA. (A)–(C) represent the steady-state kinetics of self-malonylation, self-succinylation, and self-glutarylation for PfACP, respectively. The data were analyzed by nonlinear regression analysis (r^2 = 0.99). The kinetic constants are summarized in Table 2. Similar values were obtained after analyzing the data by double reciprocal or Lineweaver-Burk plots, which are shown in the inset of the respective figures.

Table 1. Comparison of Substrate Specificity of Self-Acylation for FAS and PKS ACPs

Substrates	ActACP[a]	PfACP[b]	BnACP[b]	*E. coli* ACP
Acetyl-CoA	No	No	No	No
Malonyl-CoA	Yes	Yes	Yes	No
Succinyl-CoA	Yes	Yes	Yes	No
Glutaryl-CoA	ND	Yes	Yes	No
Butyryl-CoA	No	No	No	No
Methylmalonyl-CoA	Yes	No	No	No
Acetoacetyl-CoA	Yes	No	No	No

ND = not determined.
ActACP has been considered as representative of PKS ACPs; *E. coli* ACP has been considered as representative of ACPs that do not exhibit self-acylation property; "Yes" indicates that a particular acyl-CoA can act as a substrate for self-acylation; "No" indicates that a particular acyl-CoA cannot act as a substrate for self-acylation.
[a] [21].
[b] All experiments were carried out in triplicate and at least twice (n = 6).

We have also carried out radioactive filter-binding assays, as well as conformation-sensitive native PAGE analysis for malonyl-ACP adduct of PfACPs and BnACPs. The incorporation of radioactive [2-^{14}C]-malonate and the autoradiogram of the native PAGE shows the formation of [2-^{14}C]-malonyl-PfACP and [2-^{14}C]-malonyl-BnACP, respectively (Figures 3A–3C).

Mutational Analysis to Probe into the Residues Involved in Self-Acylation

Next, we exploited site-directed mutagenesis to probe the self-acylation behavior of the ACPs of type II fatty acid biosynthesis pathway. All the mutants were constructed, expressed in *E. coli*, and purified as described in Experimental Procedures. Successful mutagenesis

Table 2. Steady-State Rate Constants for PfACP and BnACP Self-Acylation Reactions

Substrates	K_M (μM)	k_{cat} (min^{-1})	k_{cat}/K_M (min^{-1} M^{-1}) × 10^3
PfACP			
Malonyl-CoA	23	0.194	8.43
Succinyl-CoA	73	0.164	2.2
Glutaryl-CoA	218	0.114	0.52
BnACP			
Malonyl-CoA	95	0.07	0.736
Succinyl-CoA	134	0.145	1.09
Glutaryl-CoA	377	0.174	0.46

All enzyme assays were carried out as described in Experimental Procedures. Data represent averages of four experiments carried out in triplicate.

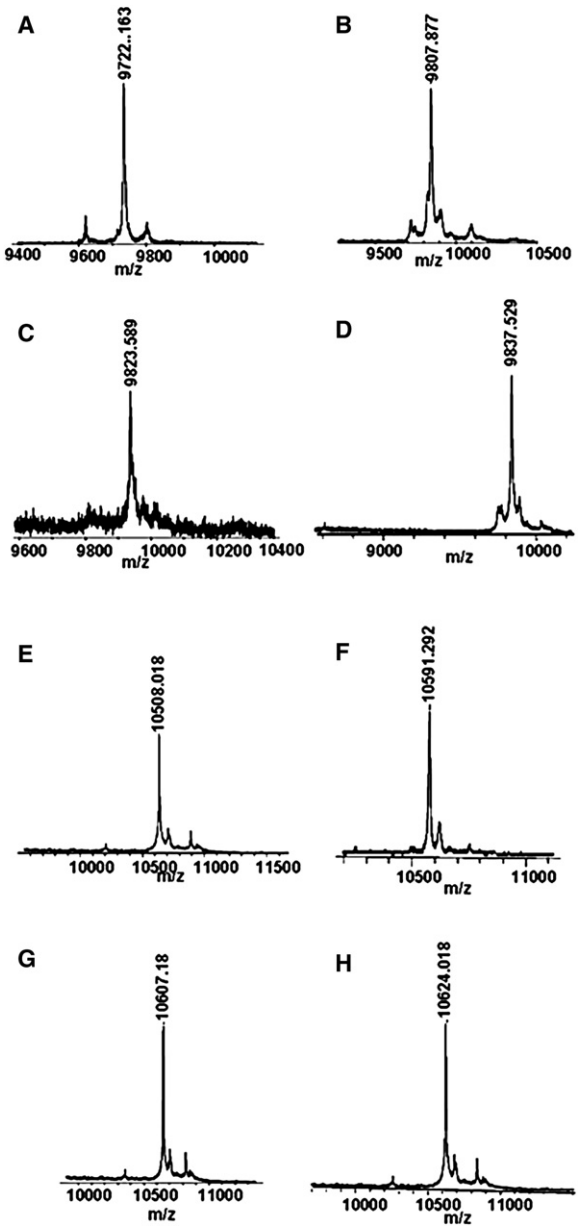

Figure 2. MALDI Mass Spectrum of Self-Malonylated, Self-Succinylated, and Self-Glutarylated Products of PfACP and BnACP

(A) Spectrum representing holo-PfACP (calculated, 9722 Da; observed, 9722.163 ± 1 Da).
(B) PfACP self-malonylation reaction showing malonyl-ACP product (calculated, 9807 Da; observed, 9807.877 ± 1 Da).
(C) PfACP self-succinylation reaction showing succinyl-ACP formation (calculated, 9823 Da; observed, 9823.589 ± 1 Da).
(D) PfACP self-glutarylation reaction showing glutaryl-ACP formation (calculated, 9837 Da; observed, 9837 ± 1 Da).
(E) Spectrum for holo-BnACP (calculated, 10,508 Da; observed, 10,508.018 ± 1 Da).
(F) BnACP self-malonylation product (calculated, 10,593 Da; observed, 10,591.292 ± 2 Da).
(G) BnACP self-succinylation product (calculated, 10,609 Da; observed, 10607.18 ± 2 Da).
(H) BnACP self-glutarylation product (calculated, 10,623 Da; observed, 10,624 ± 1 Da).

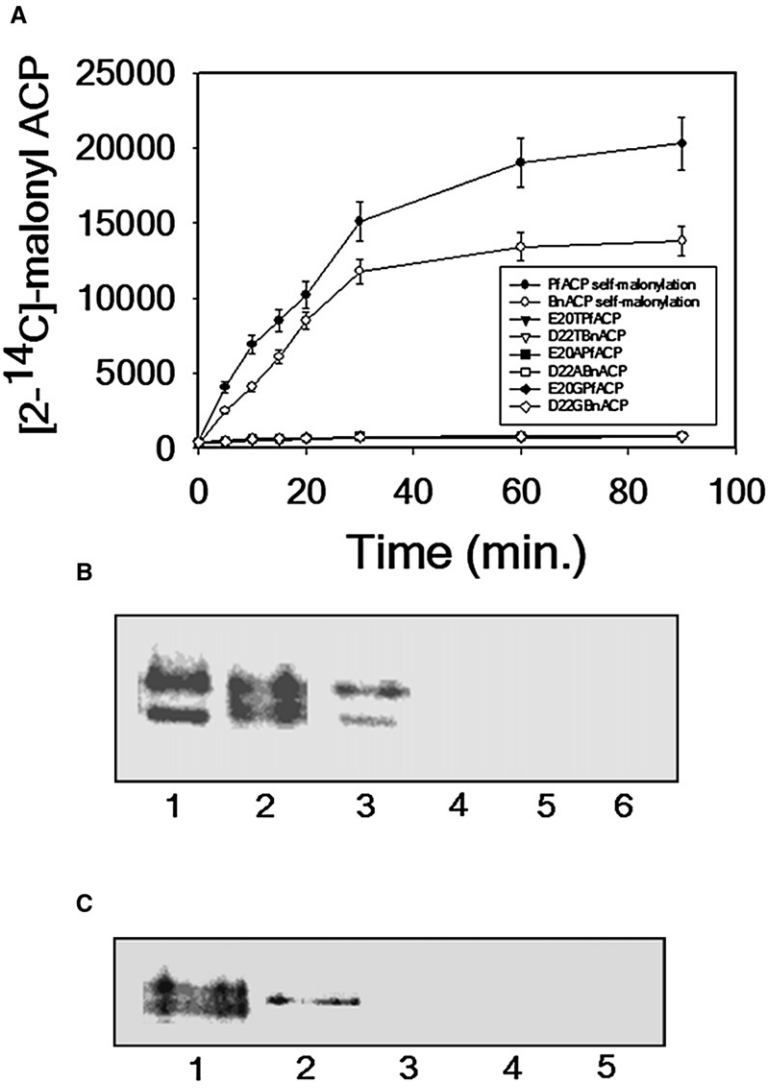

Figure 3. Self-Malonylation of Wild-Type and Mutant ACPs from *P. falciparum* and *B. napus*

(A) Self-malonylation of PfACP, BnACP, E20XPfACP, and D22XBnACP mutants (X can be threonine, glycine, or alanine) measured by the transfer of [2-^{14}C]-malonyl group from [2-^{14}C]-malonyl-CoA to ACP. The extent of self-malonylation was measured as a function of radioactive counts using a scintillation counter. Assays were performed in triplicates, and the error bars represent 95% confidence intervals. Due to low radioactivity counts in mutants, the data points of all the mutants are overlayed on each other.

(B) Conformation-sensitive native PAGE containing 0.5% urea showing the formation of malonyl-PfACP: lane 1, control reaction for Apo-PfACP (50 μM) + 20 nM [2-^{14}C]-malonyl-CoA + 100 μM malonyl-CoA + 2 μg ACPS; lane 2, self-malonylation reaction for holo-PfACP (50 μM) + 20 nM [2-^{14}C]-malonyl-CoA + 100 μM malonyl-CoA; lane 3, malonylation reaction for E20A Apo-PfACP (50 μM) + 20 nM [2-^{14}C]-malonyl-CoA + 100 μM malonyl-CoA + 2 μg ACPS; lane 4, self-malonylation reaction for E20A holo-PfACP (50 μM) + 20 nM [2-^{14}C]-malonyl-CoA + 100 μM malonyl-CoA; lane 5, self-malonylation reaction for E20T holo-PfACP (50 μM) + 20 nM [2-^{14}C]-malonyl-CoA + 100 μM malonyl-CoA; lane 6, self-malonylation reaction for E20G holo-PfACP (50 μM) + 20 nM [2-^{14}C]-malonyl-CoA + 100 μM malonyl-CoA.

(C) The formation of malonyl-BnACP: lane 1, control reaction for Apo-BnACP (50 μM) + 20 nM [2-^{14}C]-malonyl-CoA + 100 μM malonyl-CoA + 2 μg ACPS; lane 2, self-malonylation reaction for holo-BnACP (50 μM) + 20 nM [2-^{14}C]-malonyl-CoA + 100 μM malonyl-CoA; lane 3, self-malonylation reaction for D22G holo-BnACP (50 μM) + 20 nM [2-^{14}C]-malonyl-CoA + 100 μM malonyl-CoA; lane 4, self-malonylation reaction for D22A holo-BnACP (50 μM) + 20 nM [2-^{14}C]-malonyl-CoA + 100 μM malonyl-CoA; lane 5, self-malonylation reaction for D22T holo-BnACP (50 μM) + 20 nM [2-^{14}C]-malonyl-CoA + 100 μM malonyl-CoA.

was confirmed by DNA sequencing. Transfer of [2-^{14}C]-malonyl moiety from [2-^{14}C]-malonyl-CoA to ACP by ACPS (holo-ACPS from *E. coli*) was used to test the structural integrity of the mutants. The mutants that were not acylated by ACPS were thought to be structurally perturbed, and hence were not used for further studies (Figures S5A and S5B). Malonyl-PfACP is found to show two bands in conformation-sensitive native PAGE (A.M. and A.S., unpublished data), which might be due to the slowly interconverting major and minor conformations of holo-PfACP in solution [18]. The sequence identities among modular type II PKS and type II FAS ACPs are low (13%–25% in the sequences shown in Figure 4), but the sequences are highly homologous in the region that corresponds to helix II, the recognition helix in both PKS and FAS ACPs [13, 14]. Initial reports [21] suggested that salt bridges between the guanidino side chain of arginine and the carboxyl group of malonate or enolate tautomer of acetoacetate might be responsible for the self-acylation behavior. The lack of arginine residues in both PfACP and BnACP prompted us to assume that, like arginine residues in PKS ACPs, it might be the lysine residues in the FAS ACPs of *P. falciparum* and *B. napus* that are responsible for this behavior. Surprisingly, mutation of lysines 22 and 31, which are in close proximity to the 4′-PP arm of ACP to alanine, did not lead to any significant alterations in the self-acylation property. We then examined for differences in the structure(s) of ACPs exhibiting self-acylation properties to those that lack this property [21]. This led us to identify aspartate 32 in loop 1 that might be orienting the acyl-CoA moiety in a manner so as to promote a reaction with the free −SH group of the 4′-PP arm

Figure 4. Multiple Sequence Alignment of ACPs Exhibiting Self-Acylation Behavior

Actinorhodin polyketide synthase ACP (ActACP) from *Streptomyces coelicolor* (Accession no. Q02054), tetracenomycin C PKS ACP (TetACP) from *Streptomyces glaucescens* (Accession no. P12884), oxytetracycline PKS ACP (OxyACP) from *Streptomyces rimosus* (Accession no. P43677), frenolicin PKS ACP (FrenACP) from *Streptomyces roseofulvus* (Accession no. Q54996), PfACP (Accession no. O77077), BnACP (Accession no. P17650), chloroplast targeted ACP (CasACP) from *Casuarina glauca* (Accession no. P93092), chloroplast targeted ACP from *Spinacia oleracea* (SpnACP; Accession no. P23235), chloroplast targeted ACP from *Cuphea lanceolata* (CupACP; Accession no. P52412), chloroplast targeted ACP from *Hordeum vulgare* (HorACP; Accession no. P08817), ACP from *E. coli* (*E.coli* ACP; Accession no. P0A6A8), ACP from *Streptomyces coelicolor* (StrepACP; Accession no. P72393). The residue critical for the self-acylation process has been highlighted in gray. On the top are shown the secondary structural elements of actinorhodin ACP (PDB ID code 2AF8) used here as the prototype. The sequences were aligned with ClustalW.

of ACP. However, D32T mutations did not have any effect on the self-acylation properties of PfACP. Further analysis of various ACP structures implicated that threonine 54 might be helping the entry of the acyl chain of acyl-CoA into the groove between helices II and III of PfACP, thus allowing its self-acylation. This threonine was mutated to an acidic glutamate as well as a positively charged lysine, but the failure of ACPS to acylate it indicated that these mutations led to perturbation in the structure of ACPs. Hence, we explored the involvement of other residues in self-malonylation of these ACPs. Structural superposition of various ACPs exhibiting this property suggested that it might be the positioning of the 4′-PP arm, rather than the residues per se, that are responsible for this autoacylation property. Hence, we mutated leucine 40 at the start of helix II to threonine and lysine, but, again, the lack of acylation by ACPS precluded further experiments. Finally, a rigorous scrutiny of the multiple sequence alignment of amino acid sequence showed that the presence of a negatively charged residue corresponding to position 20 in PfACP is highly conserved across all ACPs exhibiting self-acylation behavior, while either a neutral or a polar amino acid was present at the corresponding position in ACPs that lack this activity (Figure 4). The alignment showed the presence of glutamate at position 20 in PfACP (Glu-20) and an aspartate at position 22 in BnACP (Asp-22). These negatively charged residues were mutated to threonine, glycine, and alanine, and self-acylation properties of E/DXT/G/A mutants were evaluated with assays identical to those performed for native PfACP and BnACP. No detectable activity was observed in these mutants even after incubating the samples with malonyl-CoA for 16 hr, demonstrating that, indeed, this residue (Glu-20 in *P. falciparum* and Asp-22 in *B. napus*) is critical for the self-acylation property of FAS ACPs. Detailed kinetic parameters of self-malonylation of wild-type and mutant ACPs are described in Table S2.

DISCUSSION

The presence of self-acylation properties in PKS ACPs has long been debated and, initially, this property was thought to be due to minor levels of *E. coli* MCAT contamination in the ACP preparations rather than specific catalytic activity of ACP [23, 24]. However, subsequent reports [25] and a recent report on self-malonylation properties of chemically synthesized actinorhodin ACP have clearly

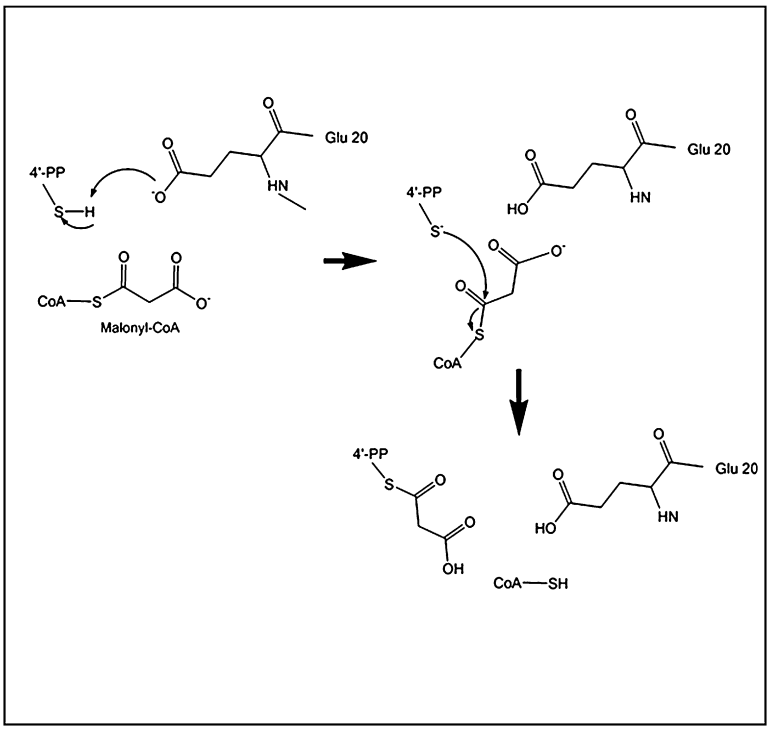

Figure 5. Proposed Catalytic Mechanism for Self-Acylation of PfACP and BnACP

Glu-20 is representative of the negatively charged residues present at this position, 4′-PP-S-H represents the 4′-phosphopantheine arm of ACP, while malonyl-CoA is representative of CoAs in the reaction. Water molecules that may shuttle protons between Glu-20, 4′-PP, and malonyl-CoA are omitted here.

established the existence of such a phenomenon in vitro [26].

The presence of this phenomenon in ACPs involved in polyketide biosynthesis was suggested to be a possible explanation for the absence of putative MCAT (malonyl CoA:ACP transacylase) in the polyketide biosynthesis gene cluster. Although, to date, no in vivo studies have been performed to confirm these observations, we have chosen ACPs involved in type II FAS from three distinct organisms—*P. falciparum*, *B. napus*, and *E. coli*—to prove that their involvement in a specific pathway does not, in itself, account for this property, but it is the presence of specific residue(s) in the protein, viz. Glu-20 in *P. falciparum* and Asp-22 in *B. napus*, that imparts them with self-malonylation ability. Kinetic analyses of substrate specificity of both PfACP and BnACP unequivocally shows that these FAS ACPs are highly selective in nature and employ only dicarboxylic acids, such as malonyl, succinyl, and glutaryl-CoAs as substrates. The lower K_M for malonyl-CoA as compared with succinyl and glutaryl-CoA shows that malonate moiety is preferred over succinate and glutarate. A comparison of the kinetic parameters shows that PfACP has almost 10-fold (23 μM) higher affinity for malonyl-CoA, while BnACP has 2- to 3-fold higher affinity (95 μM), compared with ActACP (219 μM) [20]. However, the rates of self-malonylation for these ACPs are in the same range. The observed substrate specificity of self-acylation for both FAS ACPs as well as PKS ACPs correlates well with the diverse roles they serve as members of respective biochemical pathways. PKS ACPs utilize a wide variety of substrates, ranging from dicarboxylic acids to β-keto acid thiol esters, which is consistent with the wide range of polyketides observed in nature. The lower structural diversity among fatty acids readily explains the stringent substrate specificity for self-acylation of ACPs of FAS II.

Multiple sequence alignment of ACP from various kingdoms shows that the protein is highly conserved in various forms of life. A closer examination of the sequences showed conservation of glutamate at position 20 in *P. falciparum* and corresponding glutamate/aspartate residue(s) in other ACPs exhibiting self-acylation behavior. However, they are replaced by either a positively charged or a neutral amino acid in ACPs that do not exhibit such behavior. Mutational analysis of this glutamate/aspartate residue(s) in PfACP and BnACP, respectively, confirms the importance of this residue in self-acylation reaction.

Combining the mutational results together with self-acylation activity, we propose a model of self-acylation activity whereby malonyl-/succinyl-/glutaryl-CoA first binds with the thiol (−SH) of the 4′-PP arm of PfACP/BnACP. This −SH group is then deprotonated by Glu/Asp, which promotes nucleophilic attack of the thioester of malonyl/succinyl/glutaryl-CoA by −SH of the 4′-PP arm, leading to the formation of self-acylated product. The highly flexible nature of PfACP, especially its 4′-PP arm and the loop containing Glu-20, may compensate for the relatively long distance between the reactive thiol group of 4′-PP and carboxylate of glutamate (Figure 5). We also believe that water molecules would play an important role in catalysis. This mechanism of self-acylation seems to be similar to the formation of Cys-acetylated intermediate in HAT enzymes, whereby Glu338 plays a major role in catalysis [27]. Irrespective of the exact mechanism of this reaction,

the present studies provide novel insights into the self-acylation reactions in ACPs.

Although this type of self-acylation reaction a priori casts doubt on the exact role of a functional MCAT in *P. falciparum* and *B. napus*, we believe that MCAT would be the enzyme responsible for ensuring both the specificity and efficacy permitting only malonyl-CoA to be utilized as substrate. In addition, the turnover number (k_{cat}) for the self-malonylation reaction is lower compared with the MCAT-catalyzed malonylation of ACP (A.M. et. al., unpublished data) and, thus, self-acylation might just be a fail-safe mechanism employed by these organisms.

To summarize, in addition to firmly establishing that PfACP and BnACP can undergo self-acylation, contrary to the currently held view that self-acylation is restricted only to PKS ACPs, we also provide insights into the residue that is crucial for the self-acylation behavior of type II FAS ACPs and the plausible mechanism involved therein.

SIGNIFICANCE

The presence of self-acylation process in both chloroplast targeted *Brassica napus* acyl carrier protein (ACP) and apicoplast targeted *Plasmodium falciparum* ACP further strengthens the hypothesis that the apicoplast is remnant of an ancestral photosynthetic plastid. Our observation also calls for a revision of the current thinking that self-acylation is restricted only to polyketide synthesis (PKS) type II ACPs, and instead suggests that it is a property intrinsic to a given ACP. These studies thus open a new realm to explore the possible connection between type II FAS and PKS. Also, selectivity of FAS ACPs toward dicarboxylic acids shows that these ACPs are highly evolved with regard to their substrate selectivity.

EXPERIMENTAL PROCEDURES

Materials

Oligonucleotides were purchased from Genosys, Sigma. *E. coli* DH5α cells were used during cloning of the gene. pET28a$^+$ vector (Novagen, Madison, WI) and BL21(DE3) cells (Novagen) were used for expression of the proteins. [2-^{14}C]-malonyl-CoA was purchased from American Radiolabeled Chemicals. All the other chemicals used were of the highest purity available from Sigma-Aldrich or Fluka.

Cloning of BnACP

Genomic DNA was isolated from *B. napus* seeds as previously described [28]. The chloroplast targeted BnACP (accession no. P10352) contains four exons and five introns. Exons 1 and 2 comprise the transit peptide necessary for targeting the protein to chloroplast, while exons 3 and 4 combine to form the mature functional ACP. A two-step megaprimer-based PCR method [29] was used to create final BnACP clone. In the first step, 120 bp exon 3 was PCR-amplified with primers: forward 5′-CTA GCTAGC AAACCAGAGACAGTTGAGAAAG TGTC-3′ and reverse, 5′-CTCTAAACCCATCACTATCTCAACAGTGTC GAGAGAATCTGCTCC-3′, while 123 bp exon 4 was amplified using primers, forward 5′-GCAGATTCTCTCGACACTGTTGAGATAGTGATG GGTTTAGAG-3′ and reverse 5′-CCGCTCGAGCTTCTTGGCTTGCAC GAGCTCATC-3′.

In the second step, the above-mentioned fragments were combined to give final 243 bp product with exon 1 forward and exon 2 reverse primers. The PCR cycles in both the steps consisted of an initial denaturation step of 5 min at 95°C, followed by 25 cycles of elongation at 95°C for 1 min, 55°C for 1 min, and 72°C for 15 s, followed by a final elongation step of 10 min at 72°C .The final amplified product was restriction digested and cloned between NheI and XhoI sites in pET28a$^+$ vector containing N-terminal hexa-histidine tag. pET28a$^+$-BnACP clone thus obtained was confirmed by DNA sequencing. The clone was then transformed into BL21(DE3) cells to check for overexpression of the protein.

Protein Expression and Purification

For purification of BnACP, a single colony from the BL21(DE3) plate was inoculated into 10 ml of LB broth containing kanamycin at a concentration of 30 μg/ml and allowed to grow overnight at 37°C. It was then subcultured in 500 ml of LB broth containing a similar kanamycin concentration and allowed to grow at 37°C until an A_{600} of 0.8 was achieved. The culture was then induced with 0.4 mM isopropyl-1-thio-β-D-galactopyranoside and incubated further at 37°C for 3 hr. The cells were harvested at 8000 rpm for 10 min and stored at −70°C until further use.

The cells were resuspended in lysis buffer (20 mM Tris, pH 7.5, 200 mM NaCl, 10 mM imidazole, and 10% glycerol) and lysed with a probe-type ultrasonicator and centrifuged at 15,000 rpm for 1 hr at 4°C. The supernatant, thus obtained, was loaded onto a nickel-NTA metal affinity chromatography column pre-equilibrated with the lysis buffer. The column was initially washed with lysis buffer and subsequently with lysis buffer containing 20 mM and 50 mM imidazole. Finally, the protein was eluted with lysis buffer containing 100 mM imidazole, and purity of the protein was checked by SDS-PAGE. The eluate was found to contain both apo and holo forms. Hence, to obtain holo-BnACP, it was loaded onto thiopropyl Sepharose 6B column. The fraction bound to thiopropyl Sepharose was eluted using 100 mM Tris, pH 7.5, 200 mM NaCl, 10% glycerol, containing 50 mM β-mercaptoethanol. The protein thus eluted when checked for purity by native PAGE at acidic pH showed the presence of only holo-BnACP. The concentration of holo-BnACP was determined by the method of Lowry et al. [30]. PfACP was purified as described previously [22].

Spectrophotometric Determination of Self-Acylation

The self-acylation reaction was a function of CoASH released from various acyl-CoA substrates as described previously [31]:

$$\text{Acyl-CoA} + \text{holo-ACP} \rightleftarrows \text{acyl-ACP} + \text{CoASH}$$

$$\text{CoASH} + \alpha\text{-ketoglutarate} + \text{NAD}^+ \rightleftarrows \text{succinyl-CoA} + \text{NADH} + \text{CO}_2$$

The final reaction mixture contained 50 mM phosphate buffer, pH 7.5, 1 mM EDTA, 1 mM DTT, 2 mM α-ketoglutaric acid, 0.25 mM NAD^+, 0.2 mM TPP, 15 mU/100 ml KDH, 35 μM ACP, and varying concentration from 10 to 500 μM malonyl/succinyl/glutaryl-CoA. All solutions were pre-equilibrated at 25°C and the reaction was monitored with increase in absorbance at 340 nm.

Iodoacetamide Inhibition of ACP

Free thiol (−SH) group on the phosphopantothenate arm of holo-ACP was selectively blocked with iodoacetamide. BnACP and PfACP (50 μM) were incubated with 100–500 μM iodoacetamide for 2 hr at 4°C and activity assays were then performed with [2-^{14}C]-malonyl-CoA.

Self-Malonylation with [2-^{14}C]-Malonyl-CoA

The autocatalytic malonylation of holo-ACP was also assayed with [2-^{14}C]-malonyl-CoA. Reactions were performed in 50 mM phosphate buffer, pH 7.5, containing 1 mM DTT, at 25°C. Each reaction mixture contained 20 nM [2-^{14}C]-malonyl-CoA (55 mCi/mmol) and 50 μM malonyl-CoA in a total volume of 50 μl. The reaction was initiated with 50 μM wild-type or mutant holo-ACP. Aliquots were removed at 0, 5, 10, 15, 20, 30, 60, and 90 min and quenched with 30% ice-cold trichloroacetic acid. The mixture was then pelleted and supernatant

was discarded. The pellet was resuspended in water and spotted onto Whatman 3MM filter paper. The filter papers were cut into 2.5 cm sections, placed in scintillation fluid, and counted for activity. Simultaneously, some fractions were quenched with 2× SDS-PAGE sample buffer and loaded onto a 12% native PAGE gel containing 0.5 M urea to separate ACP from malonyl-ACP. The gel was dried and [2-^{14}C]-malonyl-ACP was visualized with a PhosphorImager (Fujifilm).

MALDI Analysis of Self-Acylated Products

MALDI-time of flight (TOF) mass spectrometry was carried out for the characterization of the self-acylated products employing Ultraflex MALDI TOF/TOF (Bruker Daltonics). The reaction mixture, containing 40 μM PfACP or BnACP, 400 μM of malonyl-, succinyl-, or glutaryl-CoA in 50 mM phosphate buffer (pH 7.4), was incubated for 3 hr at 37°C and then desalted with reverse-phase C8 chromatographic media, as previously described [32]. The final pellet was suspended in 15 μl of 70% acetonitrile in water.

Multiple Sequence Alignments

Sequence alignments were performed with the program ClustalW [33] via the ClustalW web service at the European Bioinformatics Institute (http://www.ebi.ac.uk/clustalw).

Homology Modeling of BnACP

Homology models of BnACP were generated from the sequence alignments by using MODELER 8v2 [34, 35] employing *E. coli* butyryl ACP structure (PDB ID code 1L0H) as template. Five intermediate homology models were built allowing for a permutational selection of different loop candidates and side chain rotamers. The intermediate models were overlayed with ALIGN and all the intermediate models were within an rmsd of 1 Å.

Site-Directed Mutagenesis of ACP

A two-step megaprimer-based PCR method [29] was used to generate the mutants by amplifying the pET28a$^+$-BnACP or pET28a$^+$-PfACP constructs with mutation-specific primers listed in Table S1.

The PCR cycles performed were: 95°C for 3 min; 18 times each of 95°C for 30 s, 48°C for 30 s, and 72°C for 60 s; and 72°C for 10 min. The obtained products were digested and cloned into pET28a$^+$ vector and obtained mutant clones were confirmed by DNA sequencing. Mutants were expressed and purified by a similar protocol as that for their wild-type counterparts.

Supplemental Data

Supplemental Data include figures showing cloning, expression, and purification of *Brassica napus* acyl carrier protein (BnACP), graphs for the steady-state kinetics of self-malonylation, self-succinylation, and self-glutarylation of BnACP, bar diagrams of iodoacetamide-induced inhibition of self-acylation of *Plasmodium falciparum* ACPs (PfACPs) and BnACPs, autoradiogram of ACP synthase-catalyzed malonylation of wild-type and mutant PfACPs and BnACPs. It also includes a table of oligonucleotides used for site-directed mutagenesis, and a homology model of BnACP highlighting aspartate at position 22. The table also summarizes the structure-activity relationship and kinetic parameters of mutant and wild-type PfACPs and BnACPs. These materials can be found with this article online at http://www.chembiol.com/cgi/content/full/14/7/775/DC1/.

ACKNOWLEDGMENTS

This work was supported by a Centre of excellence grant from the Department of Biotechnology (DBT), Government of India to A.S. and by another DBT grant to A.S. and N.S. A.S. is a J.C. Bose Fellow of the Department of Science and Technology, Government of India. A.M. is a senior research fellow supported by the Council of Scientific and Industrial Research, Government of India.

Received: January 23, 2007
Revised: May 21, 2007
Accepted: May 25, 2007
Published: July 27, 2007

REFERENCES

1. Rock, C.O., and Cronan, J.E. (1996). *Escherichia coli* as a model for the regulation of dissociable (type II) fatty acid biosynthesis. Biochim. Biophys. Acta *1302*, 1–16.
2. Shen, B., Summers, R.G., Gramajo, H., Bibb, M.J., and Hutchinson, C.R. (1992). Purification and characterization of the acyl carrier protein of the *Streptomyces glaucescens* tetracenomycin C polyketide synthase. J. Bacteriol. *174*, 3818–3821.
3. Summers, R.G., Ali, A., Shen, B., Wessel, W.A., and Hutchinson, C.R. (1995). Malonyl-coenzyme A:acyl carrier protein acyltransferase of *Streptomyces glaucescens*: a possible link between fatty acid and polyketide biosynthesis. Biochemistry *34*, 9389–9402.
4. Kleinkauf, H., and von Dohren, H. (1990). Nonribosomal biosynthesis of peptide antibiotics. Eur. J. Biochem. *192*, 1–15.
5. Marahiel, M.A. (1992). Multidomain enzymes involved in peptide synthesis. FEBS Lett. *307*, 40–43.
6. Brozek, K.A., Carlson, R.W., and Raetz, C.R.H. (1996). A special acyl carrier protein for transferring long hydroxylated fatty acids to lipid A in *Rhizobium*. J. Biol. Chem. *27*, 132126–132136.
7. Epple, G., Van Der Drift, K.M.G.M., Thomas-Oates, J.E., and Geiger, O. (1998). Characterization of a novel acyl carrier protein, RkpF, encoded by an operon involved in capsular polysaccharide biosynthesis in *Sinorhizobium meliloti*. J. Bacteriol. *180*, 4950–4954.
8. Ritsema, T., Gehring, A.M., Stuitje, A.R., van der Drift, K.M.G.M., Dandal, I., Lambalot, R.H., Walsh, C.T., Thomas-Oates, J.E., Lugtenberg, B.J.J., and Spaink, H.P. (1998). Functional analysis of an interspecies chimera of acyl carrier proteins indicates a specialized domain for protein recognition. Mol. Gen. Genet. *257*, 641–648.
9. Smith, S., Witkowski, A., and Joshi, A.K. (2003). Structural and functional organization of the animal fatty acid synthase. Prog. Lipid Res. *42*, 289–317.
10. Waller, R.F., Keeling, P.J., Donald, R.G., Striepen, B., Handman, E., Lang-Unnasch, N., Cowman, A.F., Besra, G.S., Roos, D.S., and McFadden, G.I. (1998). Nuclear-encoded proteins target to the plastid in *Toxoplasma gondii* and *Plasmodium falciparum*. Proc. Natl. Acad. Sci. USA *95*, 12352–12357.
11. Lambalot, R.H., Gehring, A.M., Flugel, R.S., Zuber, P., LaCelle, M., Marahiel, M.A., Reid, R., Khosla, C., and Walsh, C.T. (1996). A new enzyme superfamily—the phosphopantetheinyl transferases. Chem. Biol. *3*, 923–936.
12. Elovson, J., and Vagelos, P.R. (1968). Acyl carrier protein: X. Acyl carrier protein synthetase. J. Biol. Chem. *243*, 3603–3611.
13. Weissman, K.J., Hong, H., Popovic, B., and Meersman, F. (2006). Evidence for a protein-protein interaction motif on an acyl carrier protein domain from a modular polyketide synthase. Chem. Biol. *6*, 625–636.
14. Zhang, Y.M., Wu, B., Zheng, J., and Rock, C.O. (2003). Key residues responsible for acyl carrier protein and beta-ketoacyl-acyl carrier protein reductase (FabG) interaction. J. Biol. Chem. *278*, 52935–52943.
15. Gong, H., Murphy, A., McMaster, C.R., and Byers, D.M. (2006). Neutralization of acidic residues in helix II stabilizes the folded conformation of acyl carrier protein and variably alters its function with different enzymes. J. Biol. Chem. *282*, 4494–4503.
16. Kim, Y., and Prestegard, J.H. (1990). Refinement of the NMR structures for acyl carrier protein with scalar coupling data. Proteins *4*, 377–385.

17. Andrec, M., Hill, R.B., and Prestegard, J.H. (1995). Amide exchange rates in *Escherichia coli* acyl carrier protein: correlation with protein structure and dynamics. Protein Sci. *5*, 983–993.
18. Sharma, A.K., Sharma, S.K., Surolia, A., Surolia, N., and Sarma, S.P. (2006). Solution structures of conformationally equilibrium forms of holo-acyl carrier protein (PfACP) from *Plasmodium falciparum* provides insight into the mechanism of activation of ACPs. Biochemistry *22*, 6904–6916.
19. Crump, M.P., Crosby, J., Dempsey, C.E., Parkinson, J.A., Murray, M., Hopwood, D.A., and Simpson, T.J. (1997). Solution structure of the actinorhodin polyketide synthase acyl carrier protein from *Streptomyces coelicolor* A3(2). Biochemistry *20*, 6000–6008.
20. Findlow, S.C., Winsor, C., Simpson, T.J., Crosby, J., and Crump, M.P. (2003). Solution structure and dynamics of oxytetracycline polyketide synthase acyl carrier protein from *Streptomyces rimosus*. Biochemistry *42*, 8423–8433.
21. Hitchman, T.S., Crosby, J., Byrom, K.J., Cox, R.J., and Simpson, T.J. (1998). Catalytic self-acylation of type II polyketide synthase acyl carrier proteins. Chem. Biol. *1*, 35–47.
22. Sharma, S.K., Modak, R., Sharma, S., Sharma, A.K., Sarma, S.P., Surolia, A., and Surolia, N. (2005). A novel approach for over-expression, characterization, and isotopic enrichment of a homogeneous species of acyl carrier protein from *Plasmodium falciparum*. Biochem. Biophys. Res. Commun. *330*, 1019–1026.
23. Dreier, J., Shah, A.N., and Khosla, C. (1999). Kinetic analysis of the actinorhodin aromatic polyketide synthase. J. Biol. Chem. *274*, 25108–25112.
24. Dreier, J., Li, Q., and Khosla, C. (2001). Malonyl-CoA:ACP transacylase from *Streptomyces coelicolor* has two alternative catalytically active nucleophiles. Biochemistry *40*, 12407–12411.
25. Szafranska, A.E., Hitchman, T.S., Cox, R.J., Crosby, J., and Simpson, T.J. (2002). Kinetic and mechanistic analysis of the malonyl CoA:ACP transacylase from *Streptomyces coelicolor* indicates a single catalytically competent serine nucleophile at the active site. Biochemistry *41*, 1421–1427.
26. Arthur, C.J., Szafranska, A., Evans, S.E., Findlow, S.C., Burston, S.G., Owen, P., Clark-Lewis, I., Simpson, T.J., Crosby, J., and Crump, M.P. (2005). Self-malonylation is an intrinsic property of a chemically synthesized type II polyketide synthase acyl carrier protein. Biochemistry *44*, 15414–15421.
27. Yan, Y., Harper, S., Speicher, D.W., and Marmorstein, R. (2002). The catalytic mechanism of the ESA1 histone acetyltransferase involves a self-acetylated intermediate. Nat. Struct. Biol. *9*, 862–869.
28. Alijanabi, S.M., and Martinez, I. (1997). Universal and rapid salt-extraction of high quality genomic DNA for PCR-based techniques. Nucleic Acids Res. *25*, 4692–4693.
29. Higuchi, R., Krummel, B., and Saiki, R. (1988). A general method of in vitro preparation and specific mutagenesis of DNA fragments: study of protein and DNA interactions. Nucleic Acids Res. *16*, 7351–7361.
30. Lowry, O.H., Rosebrough, N.J., Farr, A.L., and Randall, R.J. (1951). Protein measurement with the Folin phenol reagent. J. Biol. Chem. *193*, 265–275.
31. Molnos, J., Gardiner, R., Dale, G.E., and Lange, R. (2003). A continuous coupled enzyme assay for bacterial malonyl-CoA:acyl carrier protein transacylase (FabD). Anal. Biochem. *319*, 171–176.
32. Winston, R.L., and Fitzgerald, M.C. (1998). Concentration and desalting of protein samples for mass spectrometry analysis. Anal. Biochem. *262*, 83–85.
33. Thompson, J.D., Higgins, D.G., and Gibson, T.J. (1994). CLUSTAL W: improving the sensitivity of progressive multiple sequence alignment through sequence weighting, position-specific gap penalties and weight matrix choice. Nucleic Acids Res. *22*, 4673–4680.
34. Sanchez, R., and Sali, A. (1997). Evaluation of comparative protein structure modeling by MODELLER-3. Proteins (*Suppl 1*), 50–58.
35. Marti-Renom, M.A., Stuart, A., Fiser, A., Sánchez, R., Melo, F., and Sali, A. (2000). Comparative protein structure modeling of genes and genomes. Annu. Rev. Biophys. Biomol. Struct. *29*, 291–325.